Direct recycling process using Pressurized CO2 for Li-Ion battery positive electrode production scraps

Neil Hayagan, Cyril Aymonier, Laurence Croguennec, Cyril Faure, Jean-Bernard Ledeuil, Mathieu Morcrette, Rémi Dedryvère, Jacob Olchowka, Gilles Philippot

Direct recycling process using pressurized CO_2 for Li-ion batteries positive electrode production scraps

Neil Hayagan [a,b,d,e], Cyril Aymonier [a,d,e], Laurence Croguennec [a,d,e], Cyril Faure [c], Jean-Bernard Ledeuil [c,d], Mathieu Morcrette [b,d,e], Rémi Dedryvère [c,d,e], Jacob Olchowka [a,d,e*] & Gilles Philippot [a,d,e*]

a. *Univ. Bordeaux, CNRS, Bordeaux INP, ICMCB, UMR 5026, F-33600 Pessac, France*
b. *Laboratoire de Réactivité et Chimie des Solides, CNRS UMR7314, Université de Picardie Jules Verne, Hub de l'énergie, 15 rue beaudelocque, 80000 Amiens, France*
c. *IPREM, CNRS, Univ. Pau & Pays Adour, E2S UPPA, 64000, Pau, France*
d. *Réseau sur le Stockage Electrochimique de l'Energie (RS2E), CNRS FR 3459, Hub de l'Energie, Amiens, France*
e. *ALISTORE-ERI European Research Institute, CNRS FR 3104, 80039 Amiens Cedex 1, France*

Corresponding authors: jacob.olchowka@icmcb.cnrs.fr and gilles.philippot@icmcb.cnrs.fr

Abstract

This study explores a novel solvent-based delamination method that employs a mixture of triethyl phosphate (TEP), acetone, and carbon dioxide (CO_2) under pressure and temperature, for the efficient and faster direct recycling of positive electrode production scraps. Optimization of experimental conditions led to achieve a full delamination within 15 minutes at 120°C and 100 bar, with a low solvent consumption of 1.5 of TEP to electrode ratio (w/w). The CO_2 allows decreasing the viscosity of the TEP and acetone mixture and so increasing its diffusivity; favoring the binder dissolution, and accelerating the delamination process versus other reported processes. This original approach, not only enables to reduce the solvent consumption (by 6.7x), but removes the need for stirring, which is often detrimental for solvent based approaches for scaling up the process, while maintaining 100% of delamination. Subsequent to the delamination process, the active material $LiNi_{0.6}Mn_{0.2}Co_{0.2}O_2$ (NMC622) in powder form was easily and fully separated from the current collector, enabling a comprehensive characterization. A more in-depth focus on the electrochemically active material revealed that its chemical composition, crystal structure, and microstructure remained preserved throughout the recycling process. Ultimately, the electrochemical performance of the recycled NMC622 closely resembled that of pristine NMC622, affirming the promising potential of this approach.

Keywords: Li-ion batteries, direct recycling, delamination process, positive electrode, production scraps, pressurized CO_2

Introduction

Material recycling is generally perceived as a means to recover valuable elements or components from waste materials, often at their end-of-life (EOL). However, wastes are also produced during the manufacturing stage and are in that case referred to as production scraps, trimmings or cuttings. According to a report published by Circular Energy Storage, the forecasted global electrode production scraps from LIB will reach 900,000 tons per year by 2030[1]. This amount of generated production scraps is highly linked to the maturity and capacity of the production companies. Established companies with advanced production processes may reach scrap rates around 5 wt.% of electrode, while start-up companies or gigafactories starting their production could have higher scrap rates, potentially reaching up to 30 wt.%[2,3]. Although efforts are continuously made to optimize and reduce manufacturing wastes, the production scraps will always remain and require the necessity to develop efficient processes to recycle all the components they contained and efficiently reinsert them into the production chain.

Given the current surge in LIB production, it is crucial to urgently recognize electrode scraps as a distinct recyclable stream that is significantly important, requiring the development of new recycling strategies specifically tailored to scraps. These electrode scraps are composed of high-quality battery-grade materials and are generated during cutting stage, where electrodes are cut in specific sizes and shapes depending on the type of batteries required for the targeted applications. They can also encompass rejects from quality control samples, as well as other residues from LIB manufacturing processes. Unlike spent batteries, electrode production scraps possess a well-defined composition known to battery cell producers and have not undergone full battery assembly. Therefore, they have not come into contact with electrolyte, nor being cycled, thus making them safe to process, resulting in minimal degradation and superior quality compared to EOL batteries (Figure 1a). As a result, electrode production scraps are less complex and more straightforward to recycle. Henceforth, treating electrode production scraps like spent batteries would therefore be a strategic error rather than developing a dedicated recycling route, which could be more adapted and present benefits from economical and environmental point of view[4].

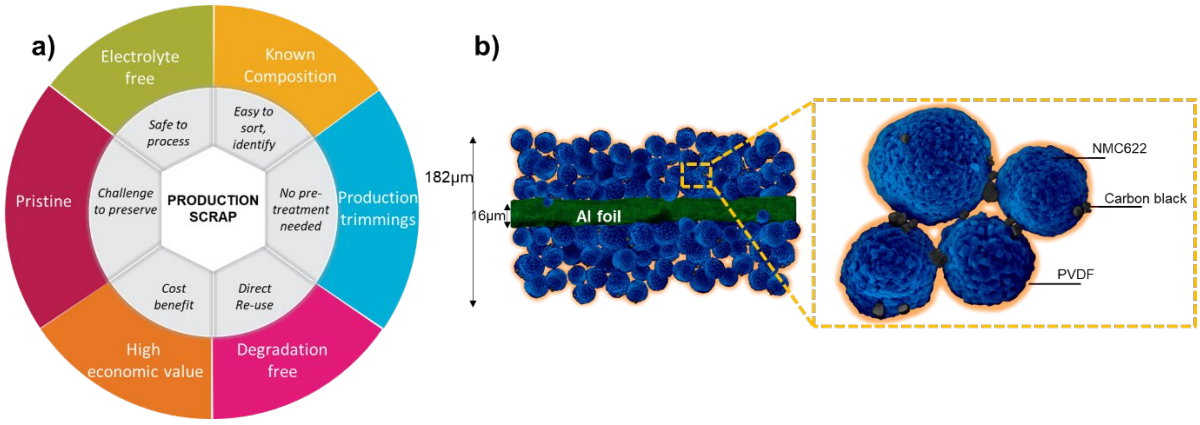

Figure 1. a) Characteristics of an electrode production scrap, especially applicable to LIB and b) Schematic of Li-ion battery positive electrode studied in this work, with detailed description of the composite components. LiNi0.6Mn0.2Co0.2O2 (NMC622) is the active material in this study,

polyvinylidene fluoride (PVDF) the binder to ensure particles cohesion on the current collector and carbon black (CB) the conductive additive to ensure electronic percolation within the electrode.

Moving away from traditional destructive methods like established pyrometallurgy and hydrometallurgy, which have limitations such as limited yield, high water and energy consumption and increased environmental impact[3,5–9], the focus shifts towards developing direct recycling processes. It offers the highest material recovery rate[10] and effectively reduces time, cost, and environmental consequences[11–13]. The success of this approach relies on the possibility of separating the various components[14] of a given waste without causing damage to preserve their pristineness and directly reintegrate a part of them into the production line. Therefore, such approach is ideal for LIB production scraps and would even allow to achieve the EU's new LIB regulation[15] for EOL batteries as each component of a battery could be potentially recovered in opposition to pyrometallurgy and hydrometallurgy that target to essentially recover the strategic elements such as lithium (Li), cobalt (Co) and nickel (Ni) that composed the positive electrode material (commonly called cathode in the battery community).

A LIB positive electrode, depicted in Figure 1b, consists of an aluminum (Al) foil coated with a composite that contains the active material, typically the $LiMO_2$ lamellar oxide with M = Ni, Co, and Mn, or Al, the carbon black and the polymer, which is most of the time PVDF. The latter acts as binder, ensuring the composite's adhesion to the current collector foil and has to be removed to release the other components of the electrode, namely the layered oxide powder and the carbon black. To do so, various methods are practiced, as presented in Table 1, among them: (i) thermal delamination techniques such as calcination and vacuum pyrolysis, (ii) mechanical stripping using cryogenic grinding or electro-mechanical methods, and (iii) chemical dissolution methods utilizing various solvents and reagents.

Table 1. Various delamination methods for LIB positive electrode with PVDF-based binder, and their characteristics. (N.I.: not indicated).

Method	Operation	Material	Temp. (°C)	Eff. (%)	Time (min)	Reference
Thermal	Calcination	Production scrap	500	97.1	90	3
	Vacuum Pyrolysis	Spent (manually separated)	600	N.I.	30	7
Mechanical	Cryogenic grinding	Spent (manually separated)	-196	87.3	5	16
	Electro-mechanical	Spent (manually separated)	590 (25kV)	93.9	N.I.	17
Chemical	Molten salt	Spent (manually separated)	160	100	20	16

	Ionic liquid	Spent (manually separated)	180	99	25	[18]

Comparing the various delamination methods outlined in Table 1, it becomes evident that the chemical method employed for binder removal exhibits the highest delamination efficiency. Moreover, it is worth noting that the thermal method requires operating at high temperatures, resulting in energy-intensive processes and the release of gaseous byproducts such as HCN, HF, CO, NO, HNCO, COF_2, and so on[3]. Dealing with the mechanical method, such approach involves peeling off the composite from the Al foil, which basically retains the binder, but leading to a maintained agglomeration of the composite[19]. In contrast, the chemical method requires a medium/solvent that enables the dissolution of the binder to separate the other components from the current collector. For instance, Bai *et al.*[20] employed TEP, for this purpose and were able to fully delaminate a 1x1 cm^2 scrap with 10:1 ratio of TEP:electrode (w/w) after one hour of stirring at 100°C in pure TEP (T_b = 211°C). Nevertheless, two main challenges have still to be addressed for the developed chemical methods: (i) the scaling up while maintaining lab scale efficiency with the necessity of high speed stirring of big volumes of highly a viscous mixtures were the solid phase consists of sheet-like (Figure1) foils[21], (ii) the proper removal of such a viscous mixture of dissolved PVDF and the solvent from the active material, that usually requires post annealing treatment at high temperatures to properly clean the surface and recover decent electrochemical performance.

In parallel, the utilization of pressurized and heated CO_2, a non-toxic, non-flammable, cheap, and environmentally friendly solvent[22–24], is well implemented in industry since the 70's, especially the field of decaffeination[25]. Recently, CO_2 as a cosolvent has gained prominence in the field of multi-material dismantling/delamination/separation[26,27]. There, when combined with a proper liquid solvent, it is possible to dissolve CO_2, by playing with the temperature and the pressure[23,24]. As a consequence, one can easily tune the overall liquid phase physical properties, leading to higher diffusion coefficient and lower viscosity, enhancing mass transfer and making such mixture an ideal medium for material impregnation and binder dissolution. Pressurized CO_2 was also used in the field of EOL LIB recycling in recent years in order to develop pretreatment steps to maximize the materials' recovery and fit with the coming regulations. The focus is on the electrolyte recovery, leading to an exfoliation of the composite active material from the current collector, and to the delamination of the positive electrode while recovering the binder [28,29].

The current study explores a novel direct recycling process for the delamination of industrial grade positive electrode production scraps through binder dissolution, combining conventional liquid solvent-based process, using TEP, and adding acetone and CO_2 as cosolvents, both miscible with TEP, to speed up the delamination process [30]. The main objective is to optimize the physicochemical properties of the solvent mixture by playing with the temperature and

pressure to tackle the two aforementioned challenges of; (i) mixture stirring and (ii) removal of dissolved PVDF and residual solvent without post annealing treatment. Experimental evidence demonstrates an enhanced electrode delamination/separation efficiency while enabling the recovery of multiple components, including the active material NMC622, the Al foil, and the PVDF binder, the latter being achieved for the first time. The preservation of the NMC622 pristineness is confirmed through a series of structural and morphological characterizations whereas electrochemical tests highlight good energy storage performance and especially excellent cycling stability similar to that of the pristine material without post annealing treatment.

Materials and methods

The studied LIB positive electrode are production scraps recovered from the production of 18650 cells on the RS2E prototyping platform at the Energy Hub, Amiens, France. The cathode slurry was made of lithium layered oxide active material NMC622 (SNMC 03006, Targray, Canada), carbon black (C-NERGY C45, Imerys, Switzerland) and PVDF binder (Polyvinylidene fluoride, Solef 5130, Solvay, Belgium), in a weight ratio of 92:4:4, and mixed with NMP (1-Methyl-2-Pyrrolidon BASF, Germany) using a Dispermat (Getzman-CE, Germany) at 1000 rpm for four hours. The slurry was double-coated on a 16 µm thick Al foil using a comma coating machine (PDL-250, People & Technology, INC., Korea) coupled with a semi-automatic winder (MTESAWM-01-A, MEDIA TECH. co., Ltd., Korea), at a coating speed of 3 m per minute, with blowing and drying temperatures of 80°C and 95°C, respectively. The electrodes underwent then a manual slitting (CLS-024T, C.I.S CO., LTD., Korea) before being calendared at 60°C with a LAP press machine (BPN-250, People & Technology, INC., Korea). The resulting electrodes have an active mass loading of 21 mg/cm^2 and a thickness of 182 µm.

Delamination and separation

A series of delamination experiments were conducted in an 18 mL batch autoclave reactor (Figure 2, actual equipment images in Figure S1). Triplicate analyses were conducted on 2 x 2 cm^2 electrode samples. For each experiment the reactor is filled with the electrode sample and defined volumes of TEP (≥ 99.8%, Sigma Aldrich, USA) and acetone (≥ 99.9%, Honeywell, France), before introducing CO_2 gas (CO_2 > 99.9995%, O_2 < 1 ppm, N_2 < 2 ppm, HC < 0.5 ppm, and CO < 0.5 ppm). To check for leaks in the system before starting the batch experiment, an initial pressure of 20 bar was added. The temperature was then gradually raised at a rate of 2°C/min to the desired value and once it was reached, the pressure setting followed. With these two parameters fixed, the reaction time began. The temperature (35°C, 70°C, 100°C or 120°C), solvent quantity (1 mL, 2.5mL, 5mL) solvents ratio (100 : 0 ; 75 :25 ; 50 :50 ;25 : 75 or 100 :0 %v/v of TEP/acetone), and time (10 min, 15 min, 30 min, 45 min or 60 min) were fine-tuned to obtain the optimized parameters for delamination and separation, at a constant pressure of 100 bar. After the time of delamination is reached, the reactor is cooled down to 50°C and was manually depressurized to atmospheric pressure. This is one of the advantages of using pressurized fluid system, where CO_2 can be easily converted back to

the gas phase and can be separated by simple depressurization. Indeed, after only 1 min sonication, the clean aluminum foil is manually recovered.

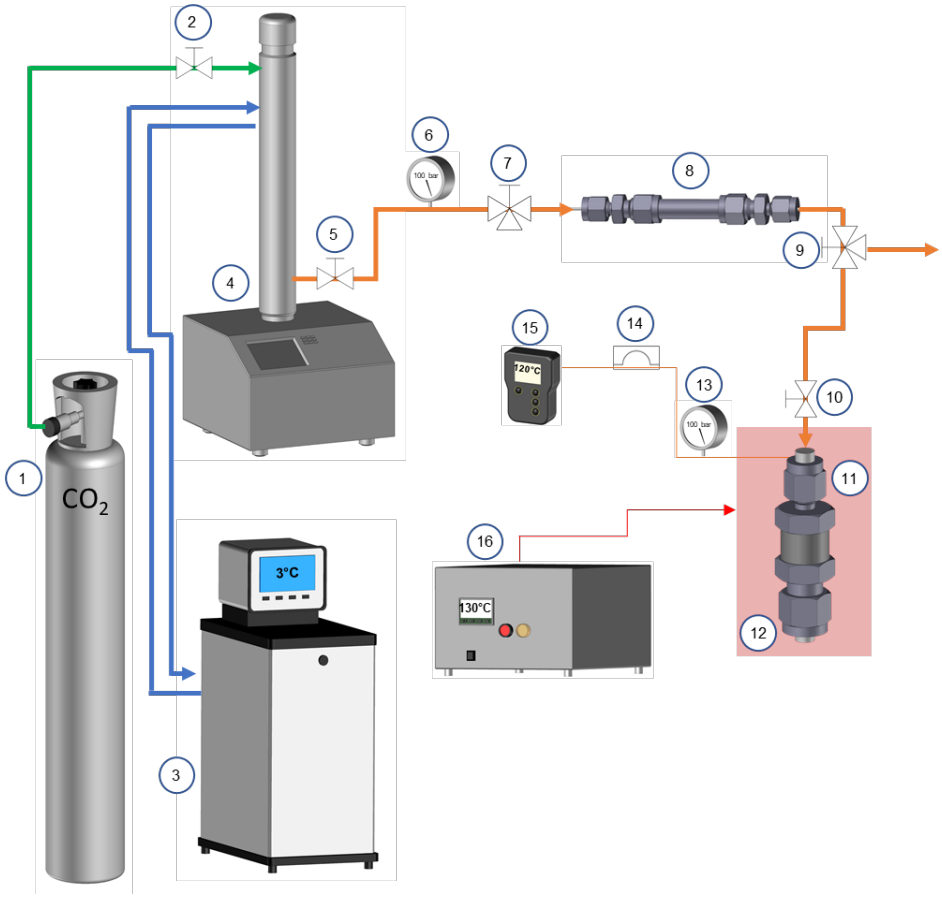

Figure 2. Schematic description of the pressurized CO_2-assisted delamination set-up :1. CO_2 cylinder bottle, 2. CO_2 inlet valve, 3. Cooling bath, 4. ISCO high pressure pump; liquid booster 5. Cooled CO_2 valve, 6. Manometer. 7. 3-way purging valve, 8. Silica water-trap filter, 9. 3-way purging valve, 10 reactor inlet valve, 11 18mL autoclave reactor, 12, oven, 13, Manometer, 14 Rupture disc, 15 Temperature display, & 16 Heating control.

After delamination, the implemented washing for components separation consists of stage processes such as sonication and vacuum filtration. The delaminated powders from the pressurized CO_2 reactor were transferred in a beaker containing 10 mL of acetone, which is then sonicated in an Elmasonic bath (S30H, Elma Schmidbauer GmbH, Germany) for 5 min, decanted and finally separated from the supernatant liquid through a vacuum filtration with 22 µm nylon filter trapping the carbon black and NMC622. This filtrate enters a pre-filled beaker containing water, where PVDF re-polymerized before being recovered after water evaporation. Since the binder acts as a glue providing adhesive force to the foil, its non-removal determines the efficiency and the recovery of the composite. Additionally, the 100% delamination also entails, 100% separation from the Al foil and therefore easily recovered.

For comparison, the delamination was also performed under stirring conditions in TEP. A 1x1 cm^2 sample was placed in a three-neck round bottom flask and was heated at 100°C for 1 h with a 1:10 wt. electrode-TEP ratio, as proposed by Bai *et al.*[20]. Then, the recovery of the cathode active material was performed in a similar way as detailed above. The powder from the stirring process was used to compare for the particle size distribution and the effect of pressurized CO_2 on recovered NMC622 microstructure.

Structural evolution evaluation via X-ray Diffraction

XRD measurements were performed using a PANanalytical Empyrean diffractometer, equipped with a Cu LFF HR (94300337310x) DK430621 X-ray tube and a Cu anode (45 kV, 40mA, Beta-filter Nickel) coupled with X'Celerator detector (RTMS type). Each diffractometer was collected from 5° to 90° (2θ) with step size of 0.0167°. Rietveld refinements of all the XRD data were performed using the FullProf Suite (January 2021 version) throughout the whole angular range. The goal here is to check for the preservation of NMC622 crystal structure which is of primary importance in direct recycling, in order to guaranty optimized properties.

Particle size and morphology tests via granulometry and SEM imaging

Particle sizes were determined using a mastersizer2000 connected to a hydro2000S auxiliary (Malvern Instruments Ltd., UK). The particles were dispersed in water under stirring and ultra-sonication with obscuration maintained at 5-6% for all measurements. Implementing dynamic light scattering, the results obtained are in volume weighted mean D [4,3]. The morphology of the recovered NMC622 loose powders was compared using Scanning Electron Microscopy (SEM). Powders for analysis were dispersed on a carbon patch and analyzed with a SEM (Tescan Essence) with SSD-EDS X-ray spectrometers (Bruker X-Flash) at 15KeV with a working distance of 5mm. No image processing was performed.

Residual polymer quantification via TGA-MS

To determine the residual amount of PVDF and carbon black in the recovered powders, thermogravimetric analysis-mass spectrometry (TGA-MS) was conducted. The thermograms were obtained using a STA449C apparatus coupled to a QMS 403 Aeolos Quadrupole-Mass Spectrometer Netzsch (Dardilly, France). Approximately 20-30 mg of sample were heated from 25 to 900°C at 5 °C.min^{-1} under synthetic air atmosphere (N_2:O_2 80:20) with a constant flow of 50mL-min^{-1}. The mass spectrometer scan is between 10 to 100m/z

Surface characterizations using XPS paired with Auger electron spectro-/microscopy (AES/SAM)

We used a Thermo Scientific ESCALAB 250 X-ray photoelectron spectroscopy (XPS) spectrometer, with a focused monochromatized Al Kα radiation (*hv*=1486.6 eV). The pressure was maintained at ~10^{-8} mbar during the analysis and charge neutralization was applied. The analyzed area of the samples was an ellipse of 450 × 900 μm^2 size. The binding energy scale was calibrated from the hydrocarbon surface contamination (C 1s peak at 284.8 eV), if not

hidden by carbon black, otherwise from the CF_2 group of PVDF (C 1s peak at 290.9 eV). For AES/SAM, electrodes were first mechanically cut, then polished by an Ar^+ ion beam in a cross-section polisher (JEOL IB-09010CP) operating at 4 keV during 2h (working pressure of 10^{-6} mbar). Polished electrodes were transferred without any air exposure into the Auger electron nanoprobe microscope (JEOL JAMP 9500F) to perform the SEM/SAM images and the AES analyses of the electrode cross sections. The analyses were carried out at a pressure < 2.10^{-9} Pa, using a primary electron beam with the following energy and current conditions: 10 keV and 8 nA, respectively.

Electrochemical performance evaluation

The recycled powders containing NMC622 with residual carbon black and PVDF are finally characterized for their electrochemical performance. At least two half cells of CR2032-type were prepared in an Ar-filled glovebox with LP30 electrolyte 1M $LiPF_6$ in 1:1 EC:DMC weight ratio (Solvionic, France), Li metal as counter electrode and the recycled powder as cathode material. The slurry formulation to prepare the positive electrode both for recycled NMC and pristine NMC was 80:10:10 in weight ratio of NMC622, carbon black and PVDF in NMP. The mixture was homogenized under stirring for 2h before being coated on an Al foil and dried in an oven at 80°C overnight. The dried sheet was then punched to get 16mm diameter discs as electrodes, those being calendared using a manual press with 5N of pressure. Active mass loading is maintained at 3.5-4.5 mg/cm^2. The cells were cycled between 2.5 and 4.3 V vs Li^+/Li at a rate of C/5 (exchange of 1 Li^+ in 5 hours) for 100 cycles using a BT-Lab (Biologic) in a GLPC mode. Another group of cells were used to perform rate capability tests at C/20, C/10,C/5, C/2, 1C, 2C, and C/10.

Results and Discussion

In this work, we use TEP and acetone combined with pressurized CO_2 to propose an efficient method to delaminate the positive electrode and selectively recover each component. Here, TEP is chosen for its ability to dissolve PVDF and its miscibility with pressurized CO_2[30]. Indeed, the Hansen solubility parameter (R_a) of TEP (1.1 MPa$^{1/2}$) is comparable to those of N-Methyl-2-pyrrolidone (NMP) (2.2 MPa$^{1/2}$) and N,N-dimethyl formamide DMF (2.4 MPa$^{1/2}$), suggesting that TEP can effectively dissolve the binder [20]. The addition of acetone and pressurized CO_2 in the process, which are miscible with TEP [30], will enable to reduce the viscosity of the TEP while enhancing its diffusivity, leading to an improved diffusion through the positive electrode and thus a more efficient binder dissolution. The use of acetone, due to its polarity, miscibility with TEP, high volatility and capacity to reduce overall viscosity, will also facilitate the TEP removal on the surface of the recovered active material after the treatment.

Delamination:

Figure 3 presents a comprehensive summary of the impact of various experimental parameters such as temperature, reaction time, and cosolvent mixture quantity on the delamination efficiency. This efficiency is inversely proportional to the amount of electrode material that remains on the current collector after the process and the determination

of the delamination efficiency is detailed in the Supporting Information (Figure S2 and Equation S1). In Figure 3a, the delamination efficiency was evaluated depending on the composition of the solvent mixture (TEP + acetone) while keeping a constant volume of 5 mL. A full delamination could be achieved after a 30 min reaction by combining pressurized CO_2 with pure TEP. As expected, using TEP without acetone as cosolvent presents challenges in the downstream cleaning process. Indeed, after the delamination process and once the suspension cooled down, the solvent becomes highly viscous, making it difficult to separate from the recovered materials[31]. The results clearly showed that the delamination efficiency was maintained intact from 100%v TEP down to 25%v within 30 min, for a constant temperature and pressure of 120°C and 100 bar of CO_2, respectively (Figure 3a). It is important to emphasize that the delamination here leads to recovering active material in powder form and not as a film.

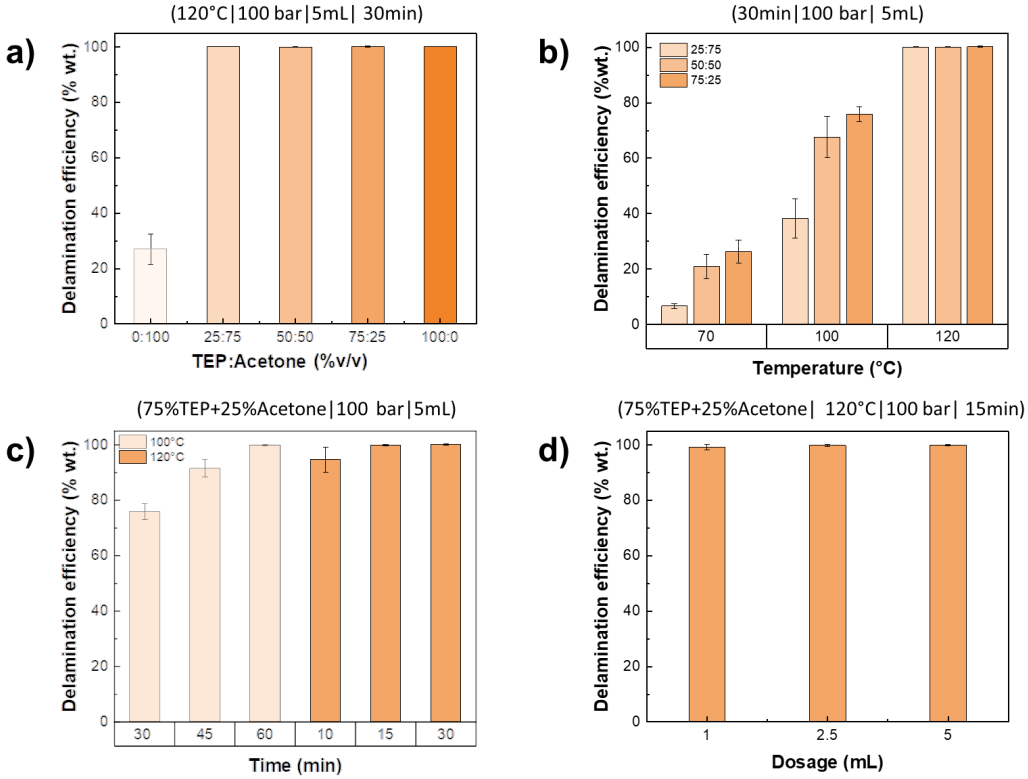

Figure 3. Delamination efficiency of a single 2x2 cm^2 (0.19g) double-side coated electrode (see Figure 1b) as a function of a) the nature and ratio of cosolvents (%v/v), b) temperature of the process, c) reaction time at fixed temperature and d) dosage effect of solvent versus electrode.

On the other hand, acetone alone cannot dissolve the binder effectively and leads to a low delamination efficiency of approximately 30 wt.%. Although acetone is able to dissolve a homopolymer PVDF (2^{nd} generation type)[32], this is not true for a PVDF Solef 5130 (3^{rd} generation type), which is a modified PVDF with higher molecular weight and lower melting point.

These first experiments validate the effectiveness of using TEP:acetone mixture with pressurized CO_2 for delaminating the positive electrode of the LIB. Apart from the solvent composition, the temperature is a crucial

parameter to successfully delaminate the electrode. Figure3b shows the delamination efficiency evolution while decreasing the temperature from 120°C down to 70°C. Note that an experiment was also performed at 35°C, but no delamination occurred. It can be observed that the delamination efficiency is globally decreasing with temperature. At 100°C with a TEP:acetone ratio of 75:25 (%v/v) only 80 wt.% of delamination is reached after a 30 min exposure time and even go down to only 30 wt.% at 70 °C, for the same exposure time. This result shows that 70°C is not high enough to have a suitable delamination, however, it is worth evaluating the influence of the exposure time at 100 and 120°C, with longer times at lower temperature and shorter times at higher temperature, as demonstrated in Figure 3c. At 100°C, the delamination efficiency increased with time. The baseline of 30 min time yielded an efficiency of 76 wt.% while 92 wt.% and 100 wt.% were recorded for 45 and 60 min, respectively. In contrast, experiments at 120°C were conducted by reducing the exposure time. A slight reduction in efficiency was observed at 10 min with a 95 wt.% efficiency, while for 15 min process, the efficiency is still 100 wt.%. From this we chose the following optimized experimental parameters: 120°C, 100 bar of CO_2, using a TEP:acetone ratio of 75:25 (%v/v) with 15 min exposure time. Note that it was experimentally shown and detailed in the supporting information (Figure S3) that it is for this specific 75:25 TEP:acetone (%v/v) ratio that the biggest amount of CO_2 is added, justifying the highest, efficiency. Once these parameters settled, the possibility to reduce the consumption of solvents by increasing the quantity of electrodes per gram of solvent was explored (Figure 3d). From the initial 5 mL (4.53 mL:g) of 75:25 TEP:acetone (%v/v) of solvent achieving a 100 wt.% delamination, the volume was gradually reduced down to 1 mL (0.91 mL:g) while keeping an excellent delamination efficiency of 99 wt.%. The reduction of solvent amount versus the amount of electrode confirms the high solubility of PVDF within TEP and provides evidence that the delamination method employed in the study is scalable, offering a significant advantage. Indeed, pressurized CO_2 assisted delamination offers advantages such as mild temperature, reduced solvent consumption, fast process, no agitation requirement, *etc.* which are of major interest when it comes to upscaling. After the process, the different components (clean aluminum foil, mixture of NMC622 with carbon black, and PVDF) can be selectively recovered through sonification and filtration as detailed in the experimental part.

Impact of the direct recycling process on the $LiNi_{0.6}Mn_{0.2}Co_{0.2}O_2$ active material

The active material is undoubtedly the most valuable component within a positive electrode, and preserving its crystal structure, bulk and surface composition, as well as its microstructure during the recycling process, is crucial for its direct reuse.

Structure and composition:

Figure 4 compares the powder X-ray diffraction (PXRD) patterns of the NMC622 recovered after delamination assisted by pressurized CO_2 with those of the pristine NCM622 material and of the manually scrapped electrode (MSE) from the current collector. This latter, which consists of the composite material of NMC622, PVDF and carbon

black, was included as a reference to observe any possible alterations in the structure resulting from electrode preparation, particularly during the calendering step.

In comparison to the pristine material, neither the electrode preparation (calendering) nor the recycling process seem to affect the layered crystal structure of the NMC622. The profile of the diffraction peaks remains unchanged and the doublets (006)/(012), (009)/(107), and (018)/(110) are well-defined with a clear splitting. All these observations suggest a good preservation of the lamellar phase with no detectable crystalline impurities, especially in the pattern collected for the recycling process.

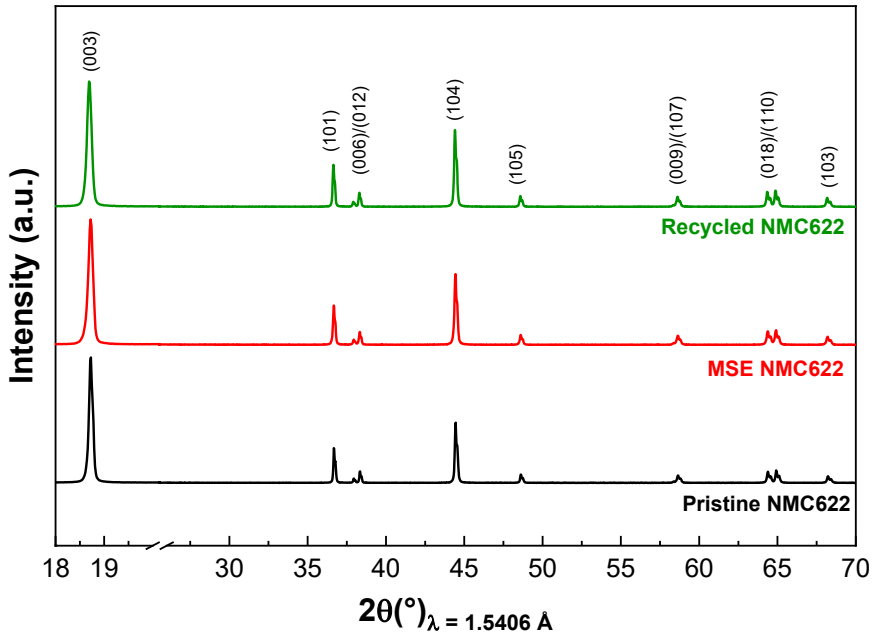

Figure 4 XRD patterns of recycled NMC622 recovered after pressurized CO_2 treatment for 15min at 120°C and 100bar, compared to that of pristine NMC622 and to manually scraped electrode (MSE) NMC622.

Structural refinements by the Rietveld method have been performed for each sample (Figures S4-S6) and a summary of their structural information is presented in Table 2. The negligible changes observed between pristine NMC622 and MSE samples could be due to the electrode preparation such as calendering, *etc.* and the presence of non-negligible amount of CB and PVDF, leading to slightly higher uncertainty for the refinement. The implemented recycling process has an insignificant impact on the cell parameters and volume (see Figures S4, S5, and S6). Moreover, no change in the crystallinity is observed. Therefore, it can be concluded that the recycling process does not affect the bulk structure of the recycled NMC622 powder.

Table 2. Structural information of NMC622 (lattice parameters, c/a ratios and cell volumes) determined from the Rietveld refinements of the XRD patterns.

Sample	a=b (Å)	c (Å)	c/a	Vol. (Å³)
Pristine NMC622	2.8704(2)	14.2218(3)	4.9547	101.474(2)
MSE NMC622	2.8712(3)	14.2211(3)	4.9530	101.529(3)
Recycled NMC622	2.8711(2)	14.2208(2)	4.9531	101.521(2)

The preservation of the NMC622 chemical composition was also confirmed via ICP-OES characterizations, which revealed that the molar ratio of Li to all transition metals (TM) is well maintained after the recycling process (Table S1). These outputs indicate that the stoichiometry is preserved and no leaching of Li occurred during the process (see supplementary information).

Quantification of residual PVDF and carbon black in the recycled NMC622 by TGA-MS:

The thermogravimetric analyses under air coupled with mass spectroscopy were conducted on the recycled powder and compared to the one obtained for MSE as shown in Figures S7a and S7b. In the case of MSE sample, depicted by the red curve, weight losses were observed across several temperature ranges, resulting in a cumulative loss of approximately 9 wt.%, consistent with the electrode formulation and the complete degradation/removal of both PVDF and carbon black. The initial weight loss up to 450°C accounts for about 4 wt.% and is attributed to the decomposition of PVDF, as confirmed by the detection of HF though mass spectroscopy. Indeed, as illustrated on the graph, the m/z=19 signal, indicative of fluorine (F) was detected between 400°C and 430°C. The second weight loss, occurring above 450°C, is attributed to the oxidation of carbon black to CO_2 and represents ≈5 wt.%. In contrast, the powder recovered after the direct recycling process exhibits an initial weight loss of 1.5 wt.% up to 450°C suggesting that a significant amount of PVDF was removed during the recycling process. Moreover, no fluorine was detected by mass spectroscopy this time, corroborating a substantial reduction in the PVDF content within the overall sample. This analysis revealed that the F compounds from the recycled NMC622 as analyzed in the exhaust gas is lower than the detection limit. This polymer amount could potentially be further reduced though optimization, *i.e.* transfer from a batch to a semi-continuous process where the solvent mixture is continuously flowed on a static sample, preventing any saturation of the solvent mixture with PVDF. The second weight loss of 5 wt.% is attributed to the carbon black as for the manually scrapped electrode. The separation of carbon black from NMC622 particles presents significant challenges due to its minute size, rendering the process difficult and practically unfeasible. Moreover, keeping a mixture of NMC622 and carbon black is not detrimental for the reuse. As long as we precisely know the amount of carbon black, it is easy to readjust the formulation of the slurry .

Microstructure and particle morphology:

Particle morphology and microstructure are crucial characteristics in powder processability for electrode preparation, which also significantly impact the long-term stability and rate capability of an electrochemically active material, hence, the success of direct recycling depends on their preservation. The SEM images presented in Figure 5 clearly demonstrate the conservation of NMC622 secondary particles spherical morphology after the recycling procedure. In fact, the particle size and size distribution exhibit remarkable similarity between the pristine material (Figure 5a) and the NMC622 recovered after CO_2-based recycling process (Figure 5c). On the other hand, the MSE powder (Figure 5b) exhibits a considerable number of aggregated secondary particles, resulting in shapeless agglomerates. This comparison confirms the effectiveness of this process allowing the removal of a majority of the binder during delamination. For an in-depth analysis, laser granulometry measurements were performed to compare precisely the particle size distribution of this series of NMC622.

In Figure 5d, the pristine powder demonstrates a unimodal distribution with an average particle size centered around 20 µm, whereas the recycled material exhibits a broader and right-skewed distribution. (Figures 5d-e)[33]. It is worth noting that the recycled powder underwent a calendering step during electrode preparation, and the applied pressure during rolling can induce deformation of the spherical particles, resulting in elongated particles[34]. Therefore, this broadening of the distribution, highlighted by the increased d_{50} and d_{90} values (Figure 5e and Table S2), is likely caused by the electrode preparation, although the presence of the residual binder maintaining the aggregation of NMC622 particles and carbon black, making it appear bigger, cannot be completely ruled out. To verify this hypothesis, we recovered the NMC622 by stirring the electrode at 100 °C for 1 hour in a solution of TEP following the procedure of Bai *et al.*[20] and found a very similar particle size distribution than for our NMC622 recovered by CO_2 approach. This confirms that the electrode preparation alters the microstructure and not the CO_2-assisted recycling process. Additionally, the recycled material displays a small peak below 5 µm revealing a population of small particles which most likely originates from fragments resulting from particles cracking during the calendering process. Given their very small size (< 100 nm), the possibility of this signal arising from carbon black particles is minimal.

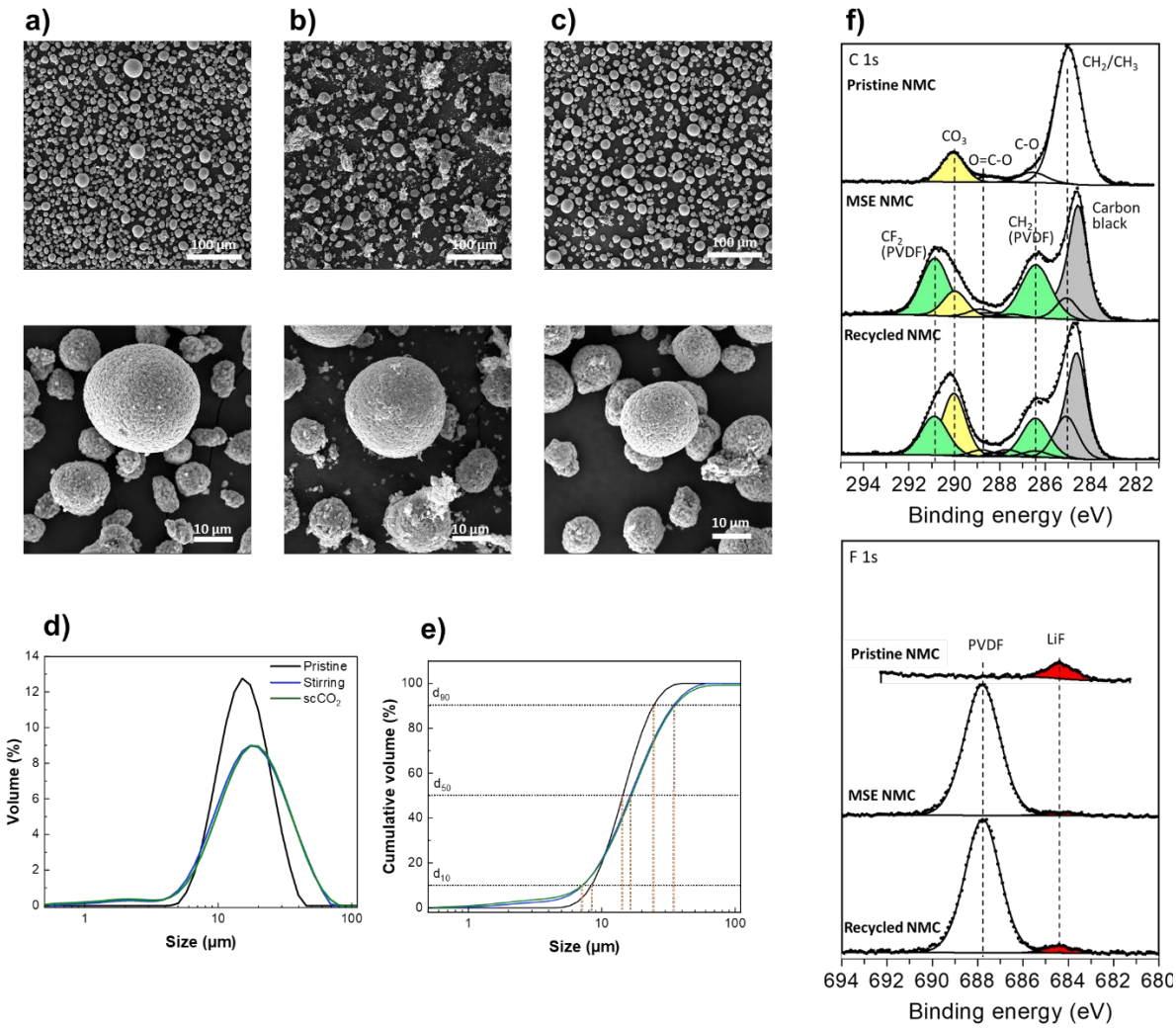

Figure 5. SEM images of powders from a) Pristine NMC622; b) MSE NMC622; c) Recycled NMC622. Particle size distribution of pristine NMC622 and recycled powders from -CO_2 conditions and recovered after stirring in TEP for 1h at 100°C according to the work of Bai et al.[20], d) dynamic light scattering showing particle size distribution, e) corresponding derived cumulative curve highlighting percentiles d10, d50, and d90 (Table S2) and f) C1s and F1s spectra of pristine NMC622, MSE NMC622 and Recycled NMC622.

Surface characteristics of the recycled NMC622:

X-ray photoelectron spectroscopy (XPS) analyses were conducted to assess the potential impact of the recycling treatment on the surface chemistry of the active material. All observable elements were investigated, including the impurities. C 1s and F 1s spectra of the pristine NMC622 powder, MSE NMC622, and recycled NMC622 are reported in Figure 5f. Other XPS spectra (transition metal 2p and 3p, Li 1s, Al 2p, O 1s and P 2p) are displayed in Figure S8. The overall spectral shapes closely resemble one another across all samples. Especially, the transition metal 2p and 3p spectra do not reveal any oxidation state modification at the surface of NMC622. The results of quantitative XPS analysis are reported in Table S3. From this analysis, the atomic % of the relevant chemical species for our study, *i.e.* the amounts of NMC622, lithium carbonate, PVDF, carbon black, other carbon-containing species, LiF, aluminum and phosphorus observed at the surface, are given in Table 3. With the exception of the presence of phosphorus (0.4

at.%) observed in the pressurized CO_2 treated sample, and attributed to traces of TEP that remain on the surface after the delamination process, no additional elements were detected on the surface of the recycled powder when compared to the pristine and manually scraped counterparts. As expected, a comparison between pristine NMC622 and the manually scraped electrode reveals a decrease of the observed atomic percentage of the active material detected at the surface due to the presence of PVDF polymer and carbon black in the electrode formulation. In contrast, the amount of Li_2CO_3 remains constant.

A comparison between the recycled and MSE samples further demonstrates the anticipated decrease in the amount of PVDF, dropping from 36 to 20 at.% at the surface, aligning well with the findings from TGA-MS and the partial removal of the binder during the delamination process. The atomic percentage of NMC622 remains similar but the Li_2CO_3 content is doubled. This latter was reported to increase when NMC, especially Ni-rich materials, are exposed to air and/or humidity[35,36]. In this case, both CO_2-assisted treatment and washing steps might have contributed to favorize the formation of Li_2CO_3. Nevertheless, the Li_2CO_3 content remains extremely low in the whole sample (not only at the surface). Besides, its precise impact on the final energy storage performance is still subject to debate and is heavily dependent on the cycling conditions[35,37,38]. Aluminum and LiF are also observed in weak amounts (coating of the active material). In MSE and recycled electrode, LiF may also arise from a slight degradation of PVDF under the X-ray beam.

Table 3. Quantification of the chemical species (atomic %) identified on the surface of Pristine NMC622, MSE NMC622 and Recycled NMC622 samples using XPS.

at. %	NMC622	Li_2CO_3	PVDF	CB	other carbon	LiF	Al	P
Pristine NMC622	40	19	0	0	19	0.6	1.6	0
MSE NMC622	6.6	21	36	18	4.0	0.8	0.2	0
Recycled NMC622	5.3	41	20	14	6.9	0.9	0.3	0.4

Electrochemical Performance

The electrochemical performance of the recycled powder was evaluated. For an accurate comparison to those of the pristine material, we prepared electrodes in the same formulation (80:10:10) with pristine NMC622 and recycled one. Galvanostatic charge/discharge performed at C/10, represented in Figure 6a, clearly demonstrate that the recycled NMC622 performs as well as the pristine material, exhibiting the same reversible capacity and a very similar polarization. On the other hand, when the current density increases to 1C (Figure 6b), the recycled material displays this time higher polarization that lowers its specific capacity due to the cut-off voltage imposed at 4.3 V vs Li^+/Li.

To further compare their energy storage performance, rate capability tests were conducted at low (C/20 and C/10), medium (C/5 and C/2) and high rates (C and 2C) as presented in Figure 6c. The discharge capacity of the recycled NMC622 is very similar to that of the pristine NMC622 throughout different current densities except at high rates of

C and 2C. However, when the low rate (C/10) was re-implemented at the end of the C-rate test, the capacity of recycled NMC622 was recovered indicating that the high rates are not detrimental to its stability and the faster decrease of capacity originates from lower kinetics. This is supported by the higher polarization encountered at 1C for the recycled powder as represented on Figure 6b.

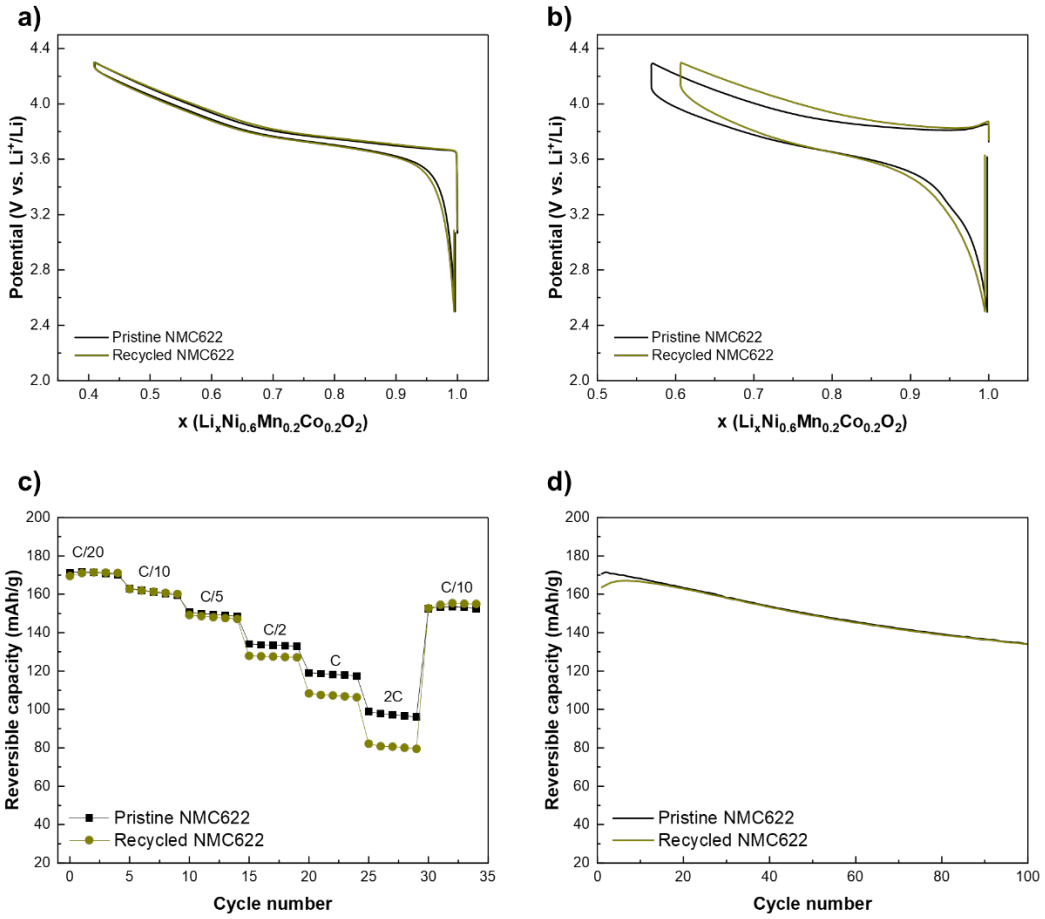

Figure 6. Galvanostatic charge/discharge (first cycle) of recycled (green curve) and pristine (black curve) NMC622 performed in half cell versus Li at a) C/10 and b) 1C. c) Rate-capability test performed at varied C-rates from C/20 to 2C with a fixed electrochemical window 2.5-4.3V vs Li^+/Li. d) Evolution of specific capacity upon 100 cycles performed at C/5 with an electrochemical window of 2.5-4.3V.

In addition to rate capability, long-term stability is extremely important and was evaluated as displayed in Figure 6d. The initial discharge specific capacity of the pristine NMC622 was 170 mAh/g, whereas the recycled NMC622 exhibited a slightly lower initial capacity of 164 mAh/g. The first cycle capacity was low for the recycled powder; but it subsequently increases until 167 mAh/g and degrades normally, following the same trend than that observed for the pristine material. This initial difference in capacity could be due to a slower electrolyte impregnation due to residual PVDF and carbon black. However, what is important is that later, the capacity profile became stable, such that the trend of the capacity degradation is highly uniform to both cells, suggesting the same material behavior which proves that the process is benign and did not alter the electrochemical stability upon cycling. This indicates that the structure is stable over the intercalation and de-intercalation of Li and was not affected by the direct

recycling process. Also, both cells revealed a capacity retention higher than 80% after 100 cycles from 2.5 - 4.3 V at a C/5 rate suggesting good electrochemical performance.

The slightly higher polarization at high current densities (> 1C rate, Figure 6c) may come from the alteration of the microstructure during the industrial processing, accentuated by the second calendaring, or due to the residual polymer which implies an optimization of the electrode formulation. To try to bring some answers, we studied the cross section of both electrodes by SEM to analyze their morphology and performed Scanning Auger Microscopy (SAM) to investigate the distribution of the different elements (F, C, O, and metals) within the electrodes.

On Figure 7, SEM images reveal that the electrode morphology from recycled NMC622 is very different from the electrode made from pristine NMC622, especially with the existence of cracks and porosity along the electrode surface, although all the experimental conditions were exactly the same. Indeed, the electrode from pristine NMC622 seems more compact with a smoother and more uniform surface than the one prepared with the recycled NMC622. Such difference in the electrode characteristics may originate from the different surface chemistries observed by XPS (presence of PVDF and carbon black already on the recycled NMC622 surface and higher amount of Li_2CO_3) that should change the rheology of the slurry prepared to cast the positive electrode. Moreover, the slight changes in particle size distribution observed by laser granulometry may also have a non-negligible impact. Therefore, it is consistent to argue that the not optimized electrode morphology for the recycled powder negatively impacts the energy storage performance, especially for fast charges/discharges when optimized electronic percolation and Li^+ diffusion are required: this could at least partially explain the difference in rate capability. Thus, an optimization of the electrode formulation is essential and needed to recover optimized performance. This point was also observed by Ouaneche *et al.*[39] in their work of direct recycling of $LiFePO_4$ although no study on electrode morphology was done to correlate the electrochemical performance.

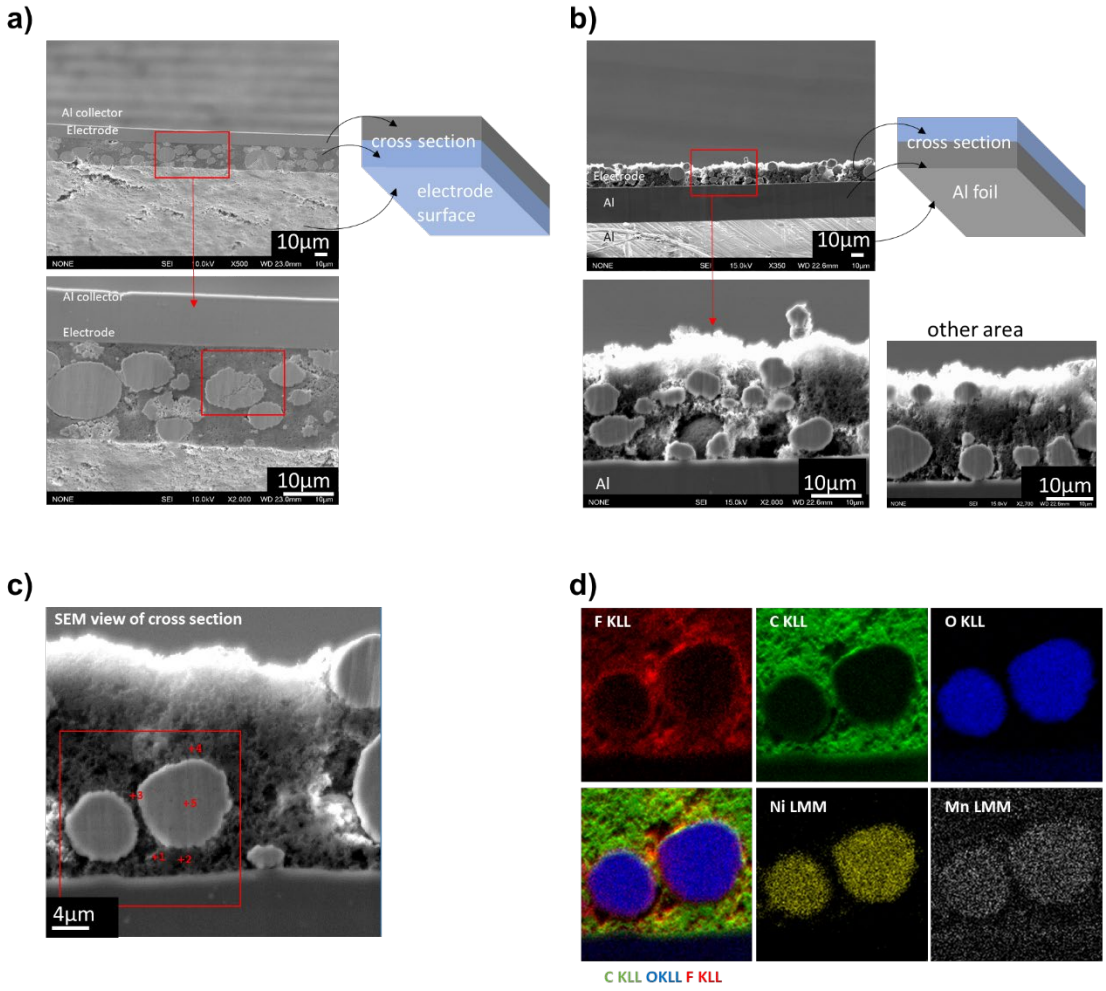

Figure 7. SEM images of cross sections of: a) pristine NMC622 electrode; b) recycled NMC622 electrode, c) SEM image of a cross section of the recycled NMC622 electrode; d) SAM images corresponding to the selected red square.

Besides, cross sections images confirm that the CO_2-assisted treatment has no impact on the NMC622 microstructure. The secondary particles of NMC622 remained dense and no cracks were observed although a pressure of 100 bar was maintained during the delamination process. Additionally, SAM reveals a rather homogeneous distribution of carbon and fluorine (PVDF) within the "porous" matrix surrounding the active materials (Figure 7d), although higher concentration of PVDF is detected at the surface of NMC622 particles, supporting the need to optimize the formulation. However, the most important point is the absence of fluorine detected in the core of the aggregates, excluding the possible transport of dissolved PVDF by the CO_2 through the porosity of secondary particles. This issue is more deeply investigated by analyzing the Auger electron spectra recorded at selected points (see Figure S9), showing that no fluorine can be evidenced at the center of the agglomerates.

PVDF and aluminum recovery

One of the notable advantages of employing the delamination via solvent dissolution method, specifically utilizing the mix-reagent scheme of TEP:acetone assisted by pressurized CO_2, is the successful recovery and possible subsequent valuation of PVDF. The delamination process involves a series of steps, sonication and vacuum filtration, which collectively contribute to enhanced separation and recovery of the components present in the positive electrode. Here, the sonication facilitates the de-agglomeration of the composite material whereas the vacuum filtration permits to separate the solid and liquid fractions, the latter containing the dissolved PVDF. Then, the polymer precipitates by introducing water in the solution and can further easily be recovered.

The integrity of the recovered polymer was further evaluated by the Fourier-Transformed Infrared spectroscopy (FTIR). Figure 8 shows that the IR spectrum of the recycled PVDF is very similar to that of fresh PVDF used in the electrode, confirming the success of the separation process while maintaining the PVDF's inherent characteristics.

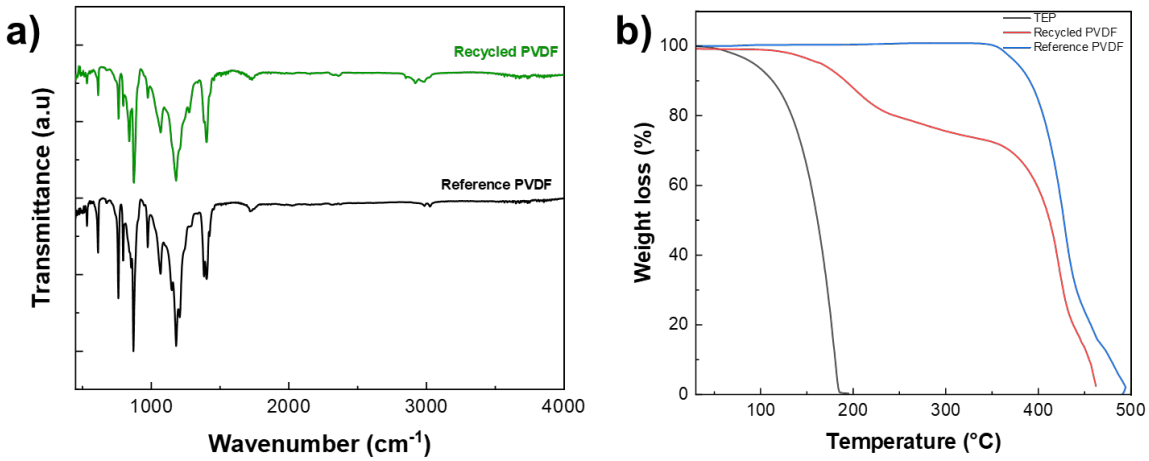

Figure 8. a) IR spectra of the recycled PVDF in comparison to the reference material and b) TGA analysis of recycled PVDF compared to the reference and to TEP.

Thermogravimetric analyses reveal that, despite the matching IR spectra displayed in Figure 8a, the recycled PVDF exhibits a different thermal stability in comparison to the reference PVDF in Figure 8b. Weight loss observed below 200°C is attributed to the presence of traces of TEP, while weight loss beyond 400°C is attributed to PVDF decomposition. The weight loss occurring between 200 and 400°C may be attributed to some alteration of the binder during the electrode preparation such as NMP swelling or other mechanisms. Despite these phenomena that need to be deeper investigated, the PVDF is effectively separated and recovered, distinguishing this method from other processes. Besides, no traces of carbon black were found with the recovered polymer.

The efficient delamination process developed in this study also allows the recovery of the Aluminum foil. 100% delamination directly correlates to 100% Al recovery. The recovery of aluminum is very important especially its

separation from active material to avoid Al contamination. Indeed, in the standard pyro- and hydrometallurgical routes, high content of Al adversely affects the extraction and separation of the metals in the positive electrode. Therefore, alkaline leaching using NaOH is usually implemented to dissolve Al as demonstrated by Ferreira *et al.*[40] and Punt *et al.*[41]. In this work, we have delaminated the composite material and recovered the Al foil intact, clean and corrosion-free as presented in the macroscopic image supported by a SEM image (Figure S10). The pits observed on the SEM images are caused by the calendering step of the electrode. Embossed holes are observed due to the applied pressure, making sure of the contact and the adhesion of the composite material to the foil. The recovered Al foil could possibly be valorized as a clean feedstock to Al production or other established Al recovery methods.

Table 4. Comparison of the different chemical delamination techniques applied to LIB positive electrode with PVDF as binder. (CAM: Cathode active material, & N.I.: not indicated)

Chemical delamination	**Solvent**	**Temp (°C)**	**Spent or scrap**	**Active mass loading (mg/cm²)/ Wt. % ratio CAM:PVDF:CB**	**Solvent: electrode (w/w)**	**Stirring**	**Eff. (%)**	**Time (min)**	**Ref**
Ionic liquid	$[BMIm][BF_4]$	180	Spent	N.I	N.I	Yes	99	25	[18]
Molten salt	$AlCl_3$-NaCl	160	Spent	N.I	10:1	Yes	99.8	20	[42]
Deep eutectic solvent	K_2CO_3-EG	100	Spent	N.I	10:1	Yes	99.3	20	[43]
Organic Solvent Dissolution	TEP	100	Scrap	19.5/ 90:5:5	10:1	Yes	100	60	[20]
		150	Spent						
	TEP+ acetone+ CO_2	120	Scrap	21.0/ 92:4:4	<1.5:1	No	100	15	This study

To further assess the impact of this study, a comparison is made with various chemical delamination techniques, summarized in Table 4. Delamination using reagents exhibits lower temperature requirements and relatively faster processing times compared to alternative techniques, as presented in Table 4. Besides the common drawback of solvent consumption for chemical delamination processes, the capability to properly mix the slurry, especially with sheet-like scraps and the solvent removal from the recycled material are the main issues. The combined used of acetone and pressurized CO_2 in this method helps mitigate these disadvantages, making it more competitive to thermal and mechanical approaches. Regarding solvent consumption, in the aforementioned table, the solvent-to-

electrode ratio is reduced to <1.5:1 w/w, minimizing solvent consumption. In the CO_2–assisted method, the solvent consumption is approximately 6.7 times lower than employing 100% TEP in stirring condition. This could be further improved by moving from batch like systems to semi-continuous ones, enabling to recirculate the solvent mixture in the system. It is worth noting that other reports provide liquid-to-solid ratios, but these systems predominantly utilize pure solvent. In contrast, this study employs a combination of TEP and acetone, with only TEP consumption considered, as it is the active solvent enabling binder dissolution.

In Table 4, all the methods present a similarity of requiring an agitation system or stirring along with the significant solvent consumption to ease the agitation. Considering that the electrodes are in a sheet-like structure, maintaining homogeneity of mixing poses challenges which is not a limitation in the CO_2 method. Additionally, stirring conditions are difficult to scale up due to electrode density and their settling in the reactor. Hence, sustaining stirring conditions for efficient delamination necessitates a substantial input of mechanical energy. In contrast, the strategy implemented in this study, employing pressurized CO_2, eliminates the need for agitation. In these conditions, CO_2 exhibits high diffusivity, hence, the CO_2 medium enables a better impregnation by the solvent mixture, ensuring better distribution of TEP and increasing contact with all PVDF matrices, thus accelerating dissolution process.

In contrast, the compared methods require a ratio of 10:1 w/w. This significant reduction in reagent consumption, coupled with the fast processing time, can be attributed to the utilization of pressurized CO_2. Finally, for chemical delamination method, in the case of pressurized processes with fluids, the solvent must be miscible with the gas carrier, CO_2 for example, on top of its ability to dissolve the binder. Furthermore, for the method to be qualified for direct recycling, it must be supported by the electrochemical performance of the recycled powder, ensuring that the solvent used is benign to NMC622. The valorization of PVDF and Al foil while preserving the properties and characteristics of the positive electrode material remains a central objective in this research.

Conclusion

This manuscript presented an innovative approach via chemical dissolution as a new direct recycling method for the LIB positive electrode scraps, which resulted to the 100% efficient delamination of the components of a positive electrode scrap. The Al foil was manually separated after the delamination process. By implementing filtration, the dissolved PVDF together with the TEP and acetone flow through, resulting to its separation from the NMC622 and carbon black mixture. The dissolved PVDF can later be recovered through reprecipitation by adding water. The recovered NMC622 and carbon black mixture was not further separated as both components are needed for the new electrode formulation. The use of pressurized CO_2 significantly improves dissolution of PVDF in TEP in terms of processing, solvent quantity consumption in mild conditions of 100 bar of CO_2 and 120°C. This process suppresses the need of stirring and could be implemented in continuous flow.

The main challenge of direct recycling to preserve and directly reuse materials is exceeded in this study, all the components, PVDF, Al foil, NMC622 and CB were successfully separated. Most importantly, the recycled NMC622 revealed pristine level properties with preserved crystal structure, morphology, and chemical composition. Long-term cycling tests revealed identical cycling behavior between the pristine and recycled NMC622 materials with similar capacity and capacity loss per cycle. Electrodes cross sections and changes in particle size distribution suggested that electrode formulation of the recycled active material would necessitate optimization, to reach fast charging electrochemical performance for electrodes made of 100% recycled material. However, we have to keep in mind that at the industrial level, only few % of recycled NMC622 will be re-injected into the production process and diluted within pristine NMC622, lowering this downside.

The optimized parameters outlined in this paper could be further evaluated by converting the setup into a semi-continuous or continuous process. For instance, the solvents utilized can be separated and recirculate the CO_2 further reducing the overall solvent consumption. This section of the article provides valuable insights of the effective utilization of pressurized CO_2 in combination with a mixture of TEP and acetone for the delamination of positive electrode production scraps, qualifying them for direct recycling. Lastly, the industrial translation of this pressurized fluids technology in multi-material composite such as the LIB electrodes is already demonstrated as this technology is used in the same range of temperature and pressure by the IDELAM company for the recycling of shoes, for instance. Implementing this technology in LIB is not limited to NMC based technologies and LIB recycling, but could be used also to other technologies such as $LiFePO_4$-based Li-ion batteries or Na-ion batteries. The TEP-acetone-CO_2 solvent system can still be used as long as the binder is PVDF. If the binder should be replaced, the technique could still be used as long as the miscibility of the solvent into the fluid is respected with a different pair of solvents that has the ability to dissolve the binder and especially benign to the cathode active material. A life cycle assessment (LCA) is being conducted to validate the impacts of this innovative process compared to others approaches in the direct recycling of LIB positive scraps but is beyond the scope of this study.

Supporting information

Details of the actual experimental set-up, delamination efficiency equation and scenarios, comparison and details of the XRD refinement data of NMC622 obtained before and after recycling, TGA-MS, XPS spectra NMC622 powder from pristine state, electrode state, and recycled state, Auger and SEM images and analyses, and ICP-OES data.

Declaration of competing interest

The authors declare that they have no known competing financial interests or personal relationships that could have appeared to influence the work reported in this paper.

Acknowledgements

As part of the DESTINY PhD Programme, the authors acknowledge the funding from the European Union's Horizon2020 research and innovation programme under the Marie Skłodowska-Curie Actions COFUND (Grant Agreement #945357), co-funded by Region Nouvelle Aquitaine (Project Region AAPR2021A-2020-11998810), from ANR through the STORE-EX Labex project ANR-10-LABX-76-01, and the REGENERATE JCJC project ANR-22-CE05-0004. This study also received financial support from the French government in the framework of the University of Bordeaux's IdEx "Investments for the Future" program / GPR PPM. We also acknowledge the CNRS.

The authors also thank the technical training and support of Monika Kezler and Jon Guisasola (ICMCB interns - exploratory investigation), Catherine Denage (ICMCB - ICP-OES, Granulometry, and TGA), Matthieu Courty (LRCS - TGA-MS), Francois Rabuel (for providing of the electrode scraps from RS2E prototyping platform), Emmanuel Petit (ICMCB - coin cell assembly, SEM), Eric Lebraud (ICMCB - XRD), Iulia Balanuta and Guillaume Aubert (ICMCB -CO_2 experiment training and Raman) and Olivier Nguyen (ICMCB - reactor set-up graphics).

Contribution of authors

Neil Hayagan conceptualization, data curation, investigation, methodology, writing-original draft, writing-review & editing, **Cyril Aymonier** conceptualization, supervision, writing-review, **Laurence Croguennec** supervision, writing-review, funding acquisition, **Cyril Faure** and **Jean-Bernard Ledeuil** exploratory investigation, **Mathieu Morcrette** supervision, writing-review, **Remi Dedryvère** supervision, writing-review, **Jacob Olchowka** conceptualization, supervision, writing-review and funding acquisition, **Gilles Philippot** conceptualization, supervision, writing-review and funding acquisition

References

(1) Circular Energy Storage Research and Consulting. *The good news about about battery production scrap*. The good news about battery production scrap. https://circularenergystorage.com/articles/2022/6/16/the-good-news-about-battery-production-scrap (accessed 2022-06-16).

(2) Gaines, L.; Dai, Q.; Vaughey, J. T.; Gillard, S. Direct Recycling R&D at the ReCell Center. *Recycling* **2021**, *6* (2), 31. https://doi.org/10.3390/recycling6020031.

(3) Hanisch, C.; Loellhoeffel, T.; Diekmann, J.; Markley, K. J.; Haselrieder, W.; Kwade, A. Recycling of Lithium-Ion Batteries: A Novel Method to Separate Coating and Foil of Electrodes. *J. Cleaner Prod.* **2015**, *108*, 301–311. https://doi.org/10.1016/j.jclepro.2015.08.026.

(4) Hayagan, N.; Gaalich, I.; Loubet, P.; Croguennec, L.; Aymonier, C.; Philippot, G.; Olchowka, J. Challenges and Perspectives for Direct Recycling of Electrode Scraps and End-of-Life Lithium-Ion Batteries. *Batteries & Supercaps* **2024**, *7* (3). https://doi.org/10.1002/batt.202400120.

(5) Georgi-Maschler, T.; Friedrich, B.; Weyhe, R.; Heegn, H.; Rutz, M. Development of a Recycling Process for Li-Ion Batteries. *J. Power Sources* **2012**, *207*, 173–182. https://doi.org/10.1016/j.jpowsour.2012.01.152.

(6) Sommerville, R.; Zhu, P.; Rajaeifar, M. A.; Heidrich, O.; Goodship, V.; Kendrick, E. A Qualitative Assessment of Lithium Ion Battery Recycling Processes. *Resources, Conservation and Recycling* **2021**, *165*, 105219. https://doi.org/10.1016/j.resconrec.2020.105219.

(7) Sun, L.; Qiu, K. Vacuum Pyrolysis and Hydrometallurgical Process for the Recovery of Valuable Metals from Spent Lithium-Ion Batteries. *Journal of Hazardous Materials* **2011**, *194*, 378–384. https://doi.org/10.1016/j.jhazmat.2011.07.114.
(8) Yang, Y.; Okonkwo, E. G.; Huang, G.; Xu, S.; Sun, W.; He, Y. On the Sustainability of Lithium Ion Battery Industry – A Review and Perspective. *Energy Storage Materials* **2021**, *36*, 186–212. https://doi.org/10.1016/j.ensm.2020.12.019.
(9) Zhou, L.-F.; Yang, D.; Du, T.; Gong, H.; Luo, W.-B. The Current Process for the Recycling of Spent Lithium Ion Batteries. *Front. Chem.* **2020**, *8*, 578044. https://doi.org/10.3389/fchem.2020.578044.
(10) Gaines, L. The Future of Automotive Lithium-Ion Battery Recycling: Charting a Sustainable Course. *Sustainable Materials and Technologies* **2014**, *1*, 2–7. https://doi.org/10.1016/j.susmat.2014.10.001.
(11) Harper, G.; Sommerville, R.; Kendrick, E.; Driscoll, L.; Slater, P.; Stolkin, R.; Walton, A.; Christensen, P.; Heidrich, O.; Lambert, S.; Abbott, A.; Ryder, K.; Gaines, L.; Anderson, P. Recycling Lithium-Ion Batteries from Electric Vehicles. *Nature* **2019**, *575* (7781), 75–86. https://doi.org/10.1038/s41586-019-1682-5.
(12) Larouche, F.; Tedjar, F.; Amouzegar, K.; Houlachi, G.; Bouchard, P.; Demopoulos, G. P.; Zaghib, K. Progress and Status of Hydrometallurgical and Direct Recycling of Li-Ion Batteries and Beyond. *Materials* **2020**, *13* (3), 801. https://doi.org/10.3390/ma13030801.
(13) Pinegar, H.; Smith, Y. R. Recycling of End-of-Life Lithium Ion Batteries, Part I: Commercial Processes. *J. Sustainable Metallurgy 2019 5:3* **2019**, *5* (3), 402–416. https://doi.org/10.1007/S40831-019-00235-9.
(14) Hayagan, N.; Aymonier, C.; Croguennec, L.; Morcrette, M.; Dedryvère, R.; Olchowka, J.; Philippot, G. A Holistic Review on the Direct Recycling of Lithium-Ion Batteries from Electrolytes to Electrodes. *J. Mater. Chem. A* **2024**. https://doi.org/10.1039/D4TA04976D.
(15) Regulation of the European Parliament and of the Council. Concerning Batteries and Waste Batteries, Repealing Directive 2006/66/EC and Amending Regulation (EU) No 2019/1020, 2020.
(16) Wang, H.; Liu, J.; Bai, X.; Wang, S.; Yang, D.; Fu, Y.; He, Y. Separation of the Cathode Materials from the Al Foil in Spent Lithium-Ion Batteries by Cryogenic Grinding. *Waste Management* **2019**, *91*, 89–98. https://doi.org/10.1016/j.wasman.2019.04.058.
(17) Tokoro, C.; Lim, S.; Teruya, K.; Kondo, M.; Mochidzuki, K.; Namihira, T.; Kikuchi, Y. Separation of Cathode Particles and Aluminum Current Foil in Lithium-Ion Battery by High-Voltage Pulsed Discharge Part I: Experimental Investigation. *Waste Management* **2021**, *125*, 58–66. https://doi.org/10.1016/j.wasman.2021.01.008.
(18) Zeng, X.; Li, J. Innovative Application of Ionic Liquid to Separate Al and Cathode Materials from Spent High-Power Lithium-Ion Batteries. *J. Hazardous Materials* **2014**, *271*, 50–56. https://doi.org/10.1016/j.jhazmat.2014.02.001.
(19) Vanderbruggen, A.; Hayagan, N.; Bachmann, K.; Ferreira, A.; Werner, D.; Horn, D.; Peuker, U.; Serna-Guerrero, R.; Rudolph, M. Lithium-Ion Battery Recycling–Influence of Recycling Processes on Component Liberation and Flotation Separation Efficiency. *ACS EST Eng.* **2022**, *2* (11), 2130–2141. https://doi.org/10.1021/acsestengg.2c00177.
(20) Bai, Y.; Essehli, R.; Jafta, C. J.; Livingston, K. M.; Belharouak, I. Recovery of Cathode Materials and Aluminum Foil Using a Green Solvent. *ACS Sustainable Chem. Eng.* **2021**, *9* (17), 6048–6055. https://doi.org/10.1021/acssuschemeng.1c01293.
(21) Ren, X.; Tong, Z.; Dai, Y.; Ma, G.; Lv, Z.; Bu, X.; Bilal, M.; Vakylabad, A. B.; Hassanzadeh, A. Effects of Mechanical Stirring and Ultrasound Treatment on the Separation of Graphite Electrode Materials from Copper Foils of Spent LIBs: A Comparative Study. *Separations* **2023**, *10* (4), 246. https://doi.org/10.3390/separations10040246.
(22) Budisa, N.; Schulze-Makuch, D. Supercritical Carbon Dioxide and Its Potential as a Life-Sustaining Solvent in a Planetary Environment. *Life* **2014**, *4* (3), 331–340. https://doi.org/10.3390/life4030331.
(23) Nikolai, P.; Rabiyat, B.; Aslan, A.; Ilmutdin, A. Supercritical CO2: Properties and Technological Applications - A Review. *J. Therm. Sci.* **2019**, *28* (3), 394–430. https://doi.org/10.1007/s11630-019-1118-4.
(24) Sihvonen, M. Advances in Supercritical Carbon Dioxide Technologies. *Trends in Food Science & Technology* **1999**, *10* (6–7), 217–222. https://doi.org/10.1016/S0924-2244(99)00049-7.

(25) Kazlas, P. T.; Novak, R. A.; Robey, R. J. Acid Treatment for Decaffeination of Coffee. WO1992003061A1, March 5, 1992. https://patents.google.com/patent/WO1992003061A1/en (accessed 2024-06-18).
(26) Aymonier, C.; Philippot, G.; Erriguible, A.; Marre, S. Materials Processing and Recycling with Near- and Supercritical CO2-Based Sovents. In *Supercritical and other high-pressure solvent systems: for extraction, reaction and material processing*; Royal Society of Chemistry, 2018; pp 304–339.
(27) Aymonier, C.; Slostowski, C. Method and Device for Dismantling Multilayer Systems Including at least One Organic Component. WO2017037260A1, March 9, 2017.
(28) Mu, D.; Liang, J.; Zhang, J.; Wang, Y.; Jin, S.; Dai, C. Exfoliation of Active Materials Synchronized with Electrolyte Extraction from Spent Lithium-Ion Batteries by Supercritical CO_2. *ChemistrySelect* **2022**, *7* (20). https://doi.org/10.1002/slct.202200841.
(29) Fu, Y.; Schuster, J.; Petranikova, M.; Ebin, B. Innovative Recycling of Organic Binders from Electric Vehicle Lithium-Ion Batteries by Supercritical Carbon Dioxide Extraction. *Resources, Conservation and Recycling* **2021**, *172*, 105666. https://doi.org/10.1016/j.resconrec.2021.105666.
(30) Pitchaiah, K. C.; Sivaraman, N.; Lamba, N.; Madras, G. Experimental Determination and Model Correlation for the Solubilities of Trialkyl Phosphates in Supercritical Carbon Dioxide. *RSC Adv.* **2016**, *6* (56), 51286–51295. https://doi.org/10.1039/C6RA10897K.
(31) Chang, J.; Zuo, J.; Zhang, L.; O'Brien, G. S.; Chung, T.-S. Using Green Solvent, Triethyl Phosphate (TEP), to Fabricate Highly Porous PVDF Hollow Fiber Membranes for Membrane Distillation. *J. Membrane Science* **2017**, *539*, 295–304. https://doi.org/10.1016/j.memsci.2017.06.002.
(32) Tan, X.; Rodrigue, D. A Review on Porous Polymeric Membrane Preparation. Part I: Production Techniques with Polysulfone and Poly (Vinylidene Fluoride). *Polymers* **2019**, *11* (7), 1160. https://doi.org/10.3390/polym11071160.
(33) Lu, X.; Zhang, X.; Tan, C.; Heenan, T. M. M.; Lagnoni, M.; O'Regan, K.; Daemi, S.; Bertei, A.; Jones, H. G.; Hinds, G.; Park, J.; Kendrick, E.; Brett, D. J. L.; Shearing, P. R. Multi-Length Scale Microstructural Design of Lithium-Ion Battery Electrodes for Improved Discharge Rate Performance. *Energy Environ. Sci.* **2021**, *14* (11), 5929–5946. https://doi.org/10.1039/D1EE01388B.
(34) Xu, J.; Ngandjong, A. C.; Liu, C.; Zanotto, F. M.; Arcelus, O.; Demortière, A.; Franco, A. A. Lithium Ion Battery Electrode Manufacturing Model Accounting for 3D Realistic Shapes of Active Material Particles. *J. Power Sources* **2023**, *554*, 232294. https://doi.org/10.1016/j.jpowsour.2022.232294.
(35) Grenier, A.; Liu, H.; Wiaderek, K. M.; Lebens-Higgins, Z. W.; Borkiewicz, O. J.; Piper, L. F. J.; Chupas, P. J.; Chapman, K. W. Reaction Heterogeneity in $LiNi_{0.8}Co_{0.15}Al_{0.05}O_2$ Induced by Surface Layer. *Chem. Mater.* **2017**, *29* (17), 7345–7352. https://doi.org/10.1021/acs.chemmater.7b02236.
(36) Li, J.; Zheng, J. M.; Yang, Y. Studies on Storage Characteristics of LiNi0.4Co0.2Mn0.4O2 as Cathode Materials in Lithium-Ion Batteries. *Journal of The Electrochemical Society* **2007**.
(37) Renfrew, S. E.; McCloskey, B. D. Quantification of Surface Oxygen Depletion and Solid Carbonate Evolution on the First Cycle of LiNi0.6Mn0.2Co0.2O2 Electrodes. *ACS Appl. Energy Mater.* **2019**, *2* (5), 3762–3772. https://doi.org/10.1021/acsaem.9b00459.
(38) Ramakrishnan, S.; Park, B.; Wu, J.; Yang, W.; McCloskey, B. D. Extended Interfacial Stability through Simple Acid Rinsing in a Li-Rich Oxide Cathode Material. *J. Am. Chem. Soc.* **2020**, *142* (18), 8522–8531. https://doi.org/10.1021/jacs.0c02859.
(39) Ouaneche, T.; Courty, M.; Stievano, L.; Monconduit, L.; Guéry, C.; Sougrati, M. T.; Recham, N. Room Temperature Efficient Regeneration of Spent LiFePO4 by Direct Chemical Lithiation. *J. Power Sources* **2023**, *579*, 233248. https://doi.org/10.1016/j.jpowsour.2023.233248.
(40) Ferreira, D. A.; Prados, L. M. Z.; Majuste, D.; Mansur, M. B. Hydrometallurgical Separation of Aluminium, Cobalt, Copper and Lithium from Spent Li-Ion Batteries. *J. Power Sources* **2009**, *187* (1), 238–246. https://doi.org/10.1016/j.jpowsour.2008.10.077.
(41) Punt, T.; Bradshaw, S. M.; van Wyk, P.; Akdogan, G. The Efficiency of Black Mass Preparation by Discharge and Alkaline Leaching for LIB Recycling. *Minerals* **2022**, *12* (6), 753. https://doi.org/10.3390/min12060753.
(42) Wang, M.; Tan, Q.; Liu, L.; Li, J. Efficient Separation of Aluminum Foil and Cathode Materials from Spent Lithium-Ion Batteries Using a Low-Temperature Molten Salt. *ACS Sustainable Chem. Eng.* **2019**, *7* (9), 8287–8294. https://doi.org/10.1021/acssuschemeng.8b06694.

(43) Hua, Y.; Xu, Z.; Zhao, B.; Zhang, Z. Efficient Separation of Electrode Active Materials and Current Collector Metal Foils from Spent Lithium-Ion Batteries by a Green Deep Eutectic Solvent. *Green Chem.* **2022**, *24* (20), 8131–8141. https://doi.org/10.1039/D2GC02844A.

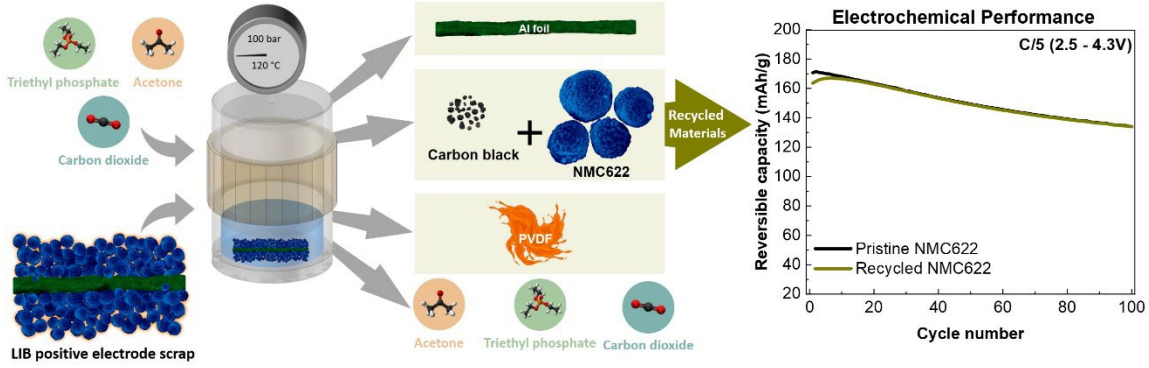

Synopsis:

Pressurized CO_2 enables a 100% efficiency delamination and separation of a production scrap Li-ion battery electrodes, recovering NMC622 with electrochemical properties comparable to pristine material. This benign, efficient process supports direct re-use, promoting sustainability by reducing waste and avoiding complex reprocessing, making it a promising solution for battery recycling.